Electronic Supplementary Material (ESI) for Journal of Materials Chemistry C.

Supporting Information:

High-performance multivalued logic circuits based on optically tunable antiambipolar transistors

Debdatta Panigrahi, Ryoma Hayakawa, Yutaka Wakayama*

International Center for Materials Nanoarchitectonics (WPI-MANA), National Institute for Materials Science (NIMS), 1-1 Namiki, Tsukuba 305-0044, Japan

Email: WAKAYAMA.Yutaka@nims.go.jp

Figure S1 (a) and (b) show the chemical structures of PhC2-BQQDI and C8-BTBT molecules, respectively. Figures S1 (c) and (d) show the atomic force microscopic (AFM) images of the PhC2-BQQDI and C8-BTBT films grown on the surface of PMMA layer.

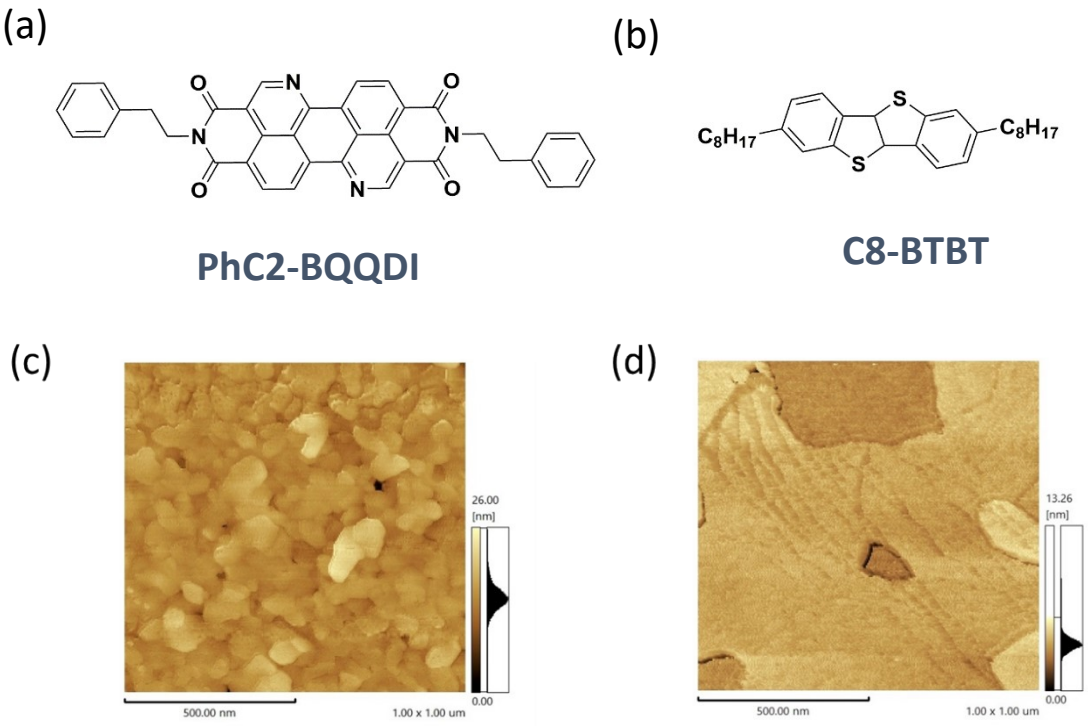

Figure S1: Chemical structures of (a) PhC2-BQQDI, (b) C8-BTBT molecules. AFM images of (c) PhC2-BQQDI and (d) C8-BTBT thin films.

Figure S2 (a) and (b) show the output characteristics of the PhC2-BQQDI and C8-BTBT transistors, respectively. The output curves of the PhC2-BQQDI transistor exhibited excellent linear behaviour at a lower V_D along a high output saturation current 15 µA upon application of $V_D = V_G = 60$ V. Along with the PhC2-BQQDI transistor, the C8-BTBT transistor also exhibited a linear increase in drain current in the lower V_D region and yielded an output current of 42 µA when $V_D = V_G = -60$ V was applied.

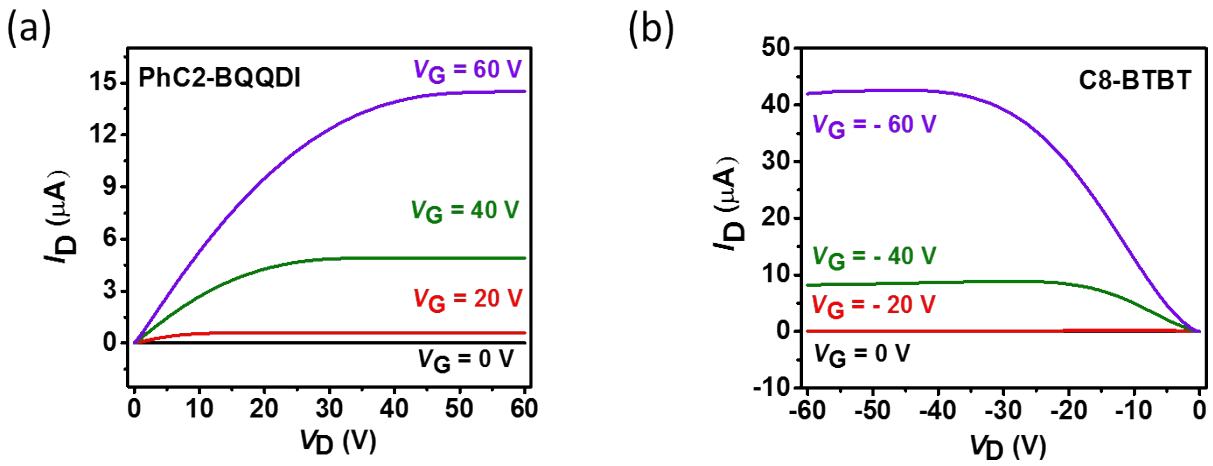

Figure S2: Output characteristics of the (a) PhC2-BQQDI and (b) C8-BTBT transistors.

Figure S3 shows the optical microscope image of the ternary inverter.

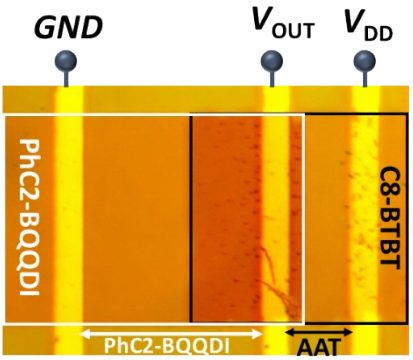

Figure S3: Optical microscope image of the ternary inverter.

Figure S4 shows the butterfly curve of the ternary inverters for the estimation of the static noise margin (SNM).

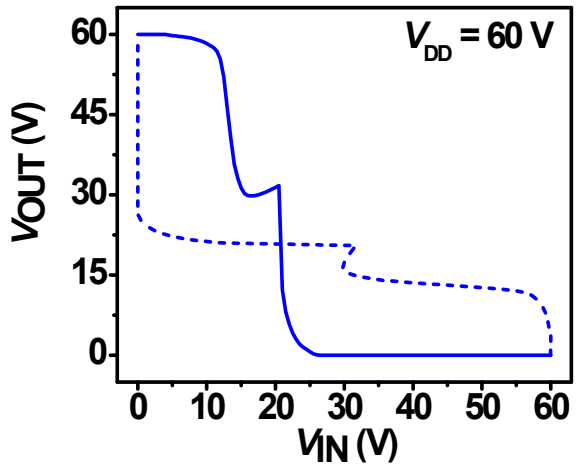

Figure S4: Butterfly curve of the ternary inverters.

Figure S5 shows the optical absorption spectra of C8-BTBT and PhC2-BQQDI semiconductors. C8-BTBT showed its absorption in ultraviolet wavelength range whereas PhC2-BQQDI showed its absorption in visible light wavelength range.

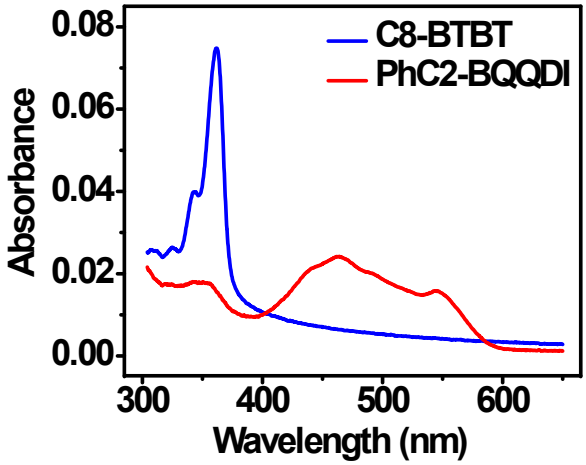

Figure S5: Optical absorption spectra of C8-BTBT and PhC2-BQQDI semiconductors.

Figure S6 (a) shows the impact of visible light on the transfer characteristics of the AATs whereas figure S6 (b) shows the impact of UV light. Due to the contrastive photosensitivity of the PhC2-BQQDI and C8-BTBT semiconductors under visible and UV light irradiation the transfer curve of the AATs exhibited a completely opposite shift.

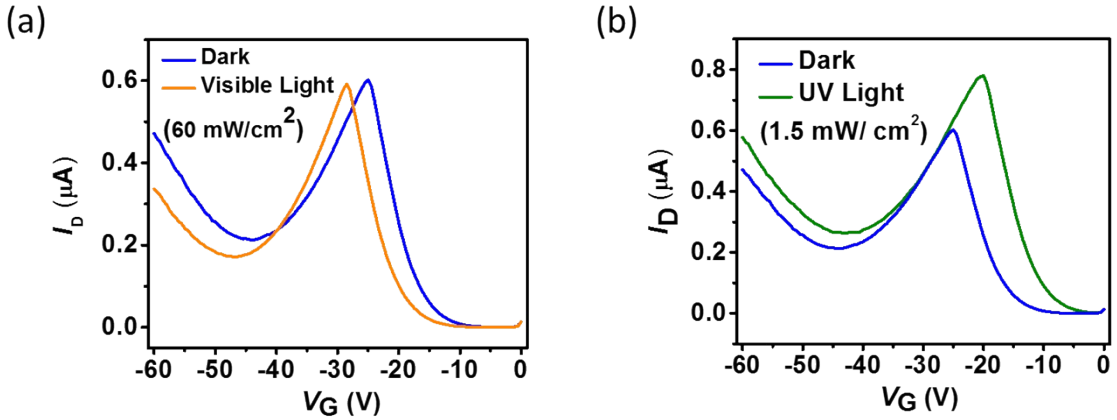

Figure S6: (a) Transfer characteristics of the AAT measured at V_D = - 60 V in the dark (blue line), and under visible light (orange line). (b) Transfer characteristics of the AAT in the dark (blue line), and under UV light (green line).

Figure S7 shows the butterfly curves of the ternary inverters under UV light intensities with 0.75 mW/cm^2 and 1 mW/cm^2. The estimated SNM values were 11.0 V and 14.4 V which were 52% and 68% of the ideal values, respectively.

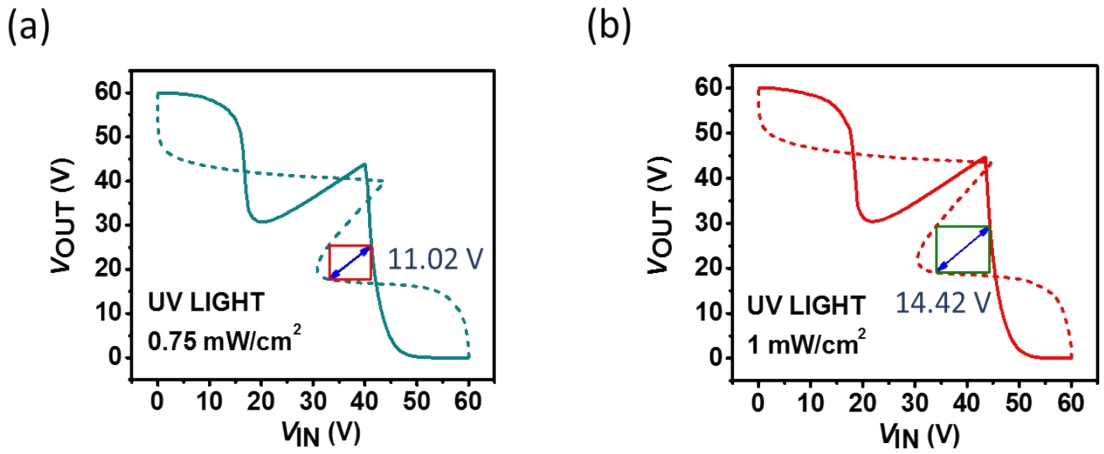

Figure S7: Butterfly curves of the ternary inverters.

Figure S8 (a) shows butterfly curve of the ternary inverters under visible light irradiation. Figure S8 (b) shows dependence of the inverter output on the visible light intensities.

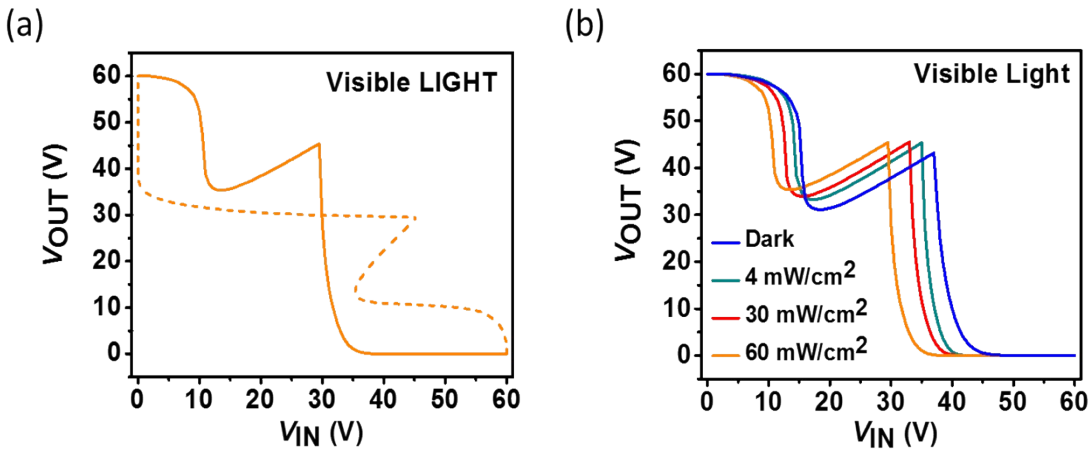

Figure S8: (a) Butterfly curve of the ternary inverters under visible light irradiation. (b) Voltage transfer characteristics of the inverters under visible light signals with various intensities.